www.czasopisma.pan.pl PAN POLSKA AKADEMIA NAUK www.journals.pan.pl
Chemical and Process Engineering 2016, 37 (3), 405-417
DOI: 10.1515/cpe-2016-0033

DYNAMICS OF PARTICLE LOADING IN DEEP-BED FILTER. TRANSPORT, DEPOSITION AND REENTRAINMENT

Rafał Przekop*, Leon Gradoń

Warsaw University of Technology, Faculty of Chemical and Process Engineering,
ul. Waryńskiego 1, 00-645 Warsaw, Poland

Deep bed filtration is an effective method of submicron and micron particle removal from the fluid stream. There is an extensive body of literature regarding particle deposition in filters, often using the classical continuum approach. However, the approach is not convenient for studying the influence of particle deposition on filter performance (filtration efficiency, pressure drop) when non-steady state boundary conditions have to be introduced. For the purposes of this work the lattice-Boltzmann model describes fluid dynamics, while the solid particle motion is modeled by the Brownian dynamics. For aggregates the effect of their structure on displacement is taken into account. The possibility of particles rebound from the surface of collector or reentrainment of deposits to fluid stream is calculated by energy balanced oscillatory model derived from adhesion theory. The results show the evolution of filtration efficiency and pressure drop of filters with different internal structure described by the size of pores. The size of resuspended aggregates and volume distribution of deposits in filter were also analyzed. The model enables prediction of dynamic filter behavior. It can be a very useful tool for designing filter structures which optimize maximum lifetime with the acceptable values of filtration efficiency and pressure drop.

Keywords: filtration, lattice Boltzmann, Brownian dynamics, multi-phase flows, porous media

1. INTRODUCTION

Deep bed filtration is an effective method of submicron and micron particle removal from the fluid stream. The quality of a filter can be described using three parameters, namely, pressure drop on the filter, its separation efficiency and retention capacity. These factors provide information about the economics of filtration and water purity. They depend mainly on particle and filter pore size and material properties of particles and filter media. There is an extensive body of literature on the initial state of filtration, when previously deposited particles have not significantly, up to this point, changed the fluid flow field and surface open for deposition. Therefore literature data cannot be applied for prediction of the lifetime of a filter. The presence of previously deposited particles produces the increase of both – filtration efficiency and pressure drop. It is worth noting that not only the total amount of deposited particles, but also their spatial distribution and structure affect filter performance (Przekop and Gradoń, 2008). Thus the development of a comprehensive model that takes into account all possible phenomena occurring during the filtration process is necessary.

Most recently published papers (Karadimos and Ocone, 2003; Przekop and Podgórski, 2004; Przekop et al., 2004; Sztuk et al., 2012; Wang et al., 2006) consider particle deposition on the collector using the classical continuum approach. This approach can be efficiently used only for the initial stage of filtration, when previously deposited particles have not as yet significantly changed the fluid flow field

*Corresponding author, e-mail: rprzekop@ichip.pw.edu.pl

and surface open for deposition. Some papers (Dunnett and Clement, 2006; Dunnett and Clement, 2012) take into account deposit growth, but the approach requires making assumptions of deposit structure. The important advantage in deep bed filtration modeling was introduction of lattice gas automata (Biggs et al., 2003) and lattice-Boltzmann method (Long and Hilpert, 2009), that allows to take into account the geometry of flow change due to deposition of suspended particles. Biggs et al. (2003) have studied the deposition of particles in 2D constriction unit cell and random 2D porous medium. Long and Hilpert (2009) have studied the filtration in sphere packings, using advection-diffusion equation for transport of particles. By performing the set of numerical experiments the authors have developed the correlation for diffusional efficiency, but interception and sedimentation efficiency could be only obtained by employing terms from unit cell correlations. The authors have also reported the numerical instabilities for the fluid velocities higher than those of μm/s order.

The growth of deposits causes the decrease of local porosity and thus the increase of local fluid velocity and shear stress that may lead to the re-entrainment of single particles or aggregates. The phenomenon is not necessarily negative as resuspended particles may redeposit at the deeper layers of a filter structure, which results in a more uniform distribution of deposits through the filter and prevents the filter from clogging which boosts the filter lifetime. In this work we combine lattice-Boltzmann hydrodynamics, Brownian dynamics method for particles displacement and energy balanced model of adhesion to find a comprehensive model that describes the mentioned above phenomena and may predict their effect on filter performance e.g. deposition efficiency, volume distribution of deposits or pressure drop.

2. THEORETICAL BACKGROUND

2.1. Filter structure model

The real structure of pores formatting a filter is too complicated for direct modeling. In this work we have decided to examine the constricted tube model. The model was proposed by Payatakes et al. (1973). The geometry of a unit cell, presented in Fig. 1, is described by the inlet and outlet radii of the tube, the tube radius in the narrowest cross section, the tube length and its orientation angle. The model accounts for the fluid velocity variations and phenomena related to converging/diverging character of flow within pores.

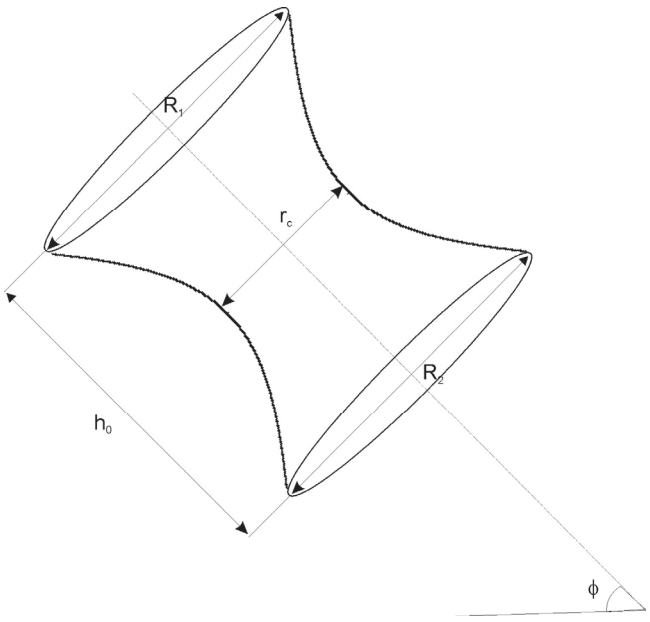

Fig. 1. The geometry of unit cell

The overall structure of a porous medium is modeled as a cubic lattice of unit cells (Skouras et al., 2004). The cell inclination was chosen to be equal $\phi = \sin^{-1}(1/\sqrt{3})$ so as not to favor flow along any of the main directions. (Fig. 2).

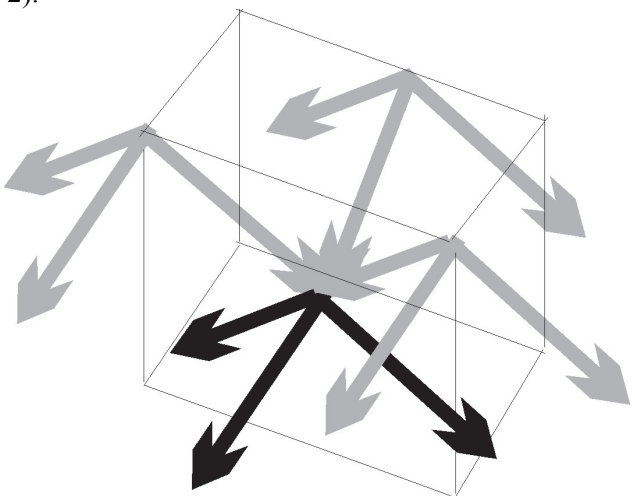

Fig. 2. Flow directions within the unit cells of network

2.2. Lattice-Boltzmann model of hydrodynamics

Complete information on the statistical description of a fluid at, or near, its thermal equilibrium is assumed to be contained in the one-particle phase-space distribution function f (*x, t,* □*)* for atomic constituents of the system. The variables *x* and *t* are the space and time coordinates of the atoms and □ stands for all other phase-space coordinates e.g. momentum, momentum flux. Since collisions preserve conservation laws, by integration of Boltzmann equation over the continuity equation and momentum tensor, an equation describing the macrodynamics of a system can be derived. To build a cellular-space picture with collective motion dynamics predicted by Navier-Stokes equation, a lattice on which particles move, collision rules and other restrictions characteristic for a chosen model should be defined. In this work a 3-D lattice with 19 allowed movement directions usually referred to as D3Q19, was used. The allowed directions, aside a particle at rest, are the middle of faces and edge.

The evolution of the system is described by the expression:

$$f\left(\bar{x}+e_i,\bar{t}+1\right)-f\left(\bar{x},\bar{t}\right)=\Omega\left(f\right) \tag{1}$$

The outcome of a collision can be approximated by assuming that the momentum of interacting particles will be redistributed at some constant rate toward an equilibrium distribution $f_i^{eq}(x,t)$ (Qian et al., 1992). This simplification is called the single-time-relaxation approximation or lattice-BGK (Bhatnagar-Gross-Krook) and can be given by:

$$f\left(\bar{x}+e_i,\bar{t}+1\right)-f\left(\bar{x},\bar{t}\right)=\Omega\left(f\right) \tag{2}$$

In the single-time-relaxation approximation, the momentum distribution at each lattice site is forced toward the equilibrium distribution at each time step. In the absence of external forces, the equilibrium distribution of a state with zero net momentum is just equal to momentum in each direction. The rate of change toward equilibrium is $1/\bar{\tau}$, the inverse of relaxation time, and is chosen to produce the desired value of fluid viscosity.

$$\bar{v}=\frac{\bar{c}_s^{\,2}}{2}\left(2\bar{\tau}-1\right) \tag{3}$$

The equilibrium distribution $f_i^{eq}(x,t)$ is given as follows:

$$f_{i^{eq}} = \overline{\rho}\,\alpha_i\left(1+\frac{e_i\overline{u}}{\overline{c}_s^{\,2}}+\frac{1}{2}\left(\frac{e_i\overline{u}}{\overline{c}_s^{\,2}}\right)^2-\frac{\overline{u}^2}{2\overline{c}_s^{\,2}}\right) \tag{4}$$

where a_i are the model dependent constants. The values of parameters in Eq. (4) for different lattice geometries can be found in Masselot (2000). The values of a_i's for a particle at rest, the middles of faces and edges are 1/3, 1/18 and 1/36, respectively. The speed of sound, $\overline{c}_s$, is equal to $\sqrt{1/3}$.

The equation of state for a discrete space has the following form:

$$\overline{P} = \overline{c}_s^{\,2}\overline{\rho} \tag{5}$$

2.3. Brownian dynamics particle motion model

Determination of the structures of deposited particles in a filter requires the knowledge of an individual particle history, its position and velocity vectors. The Lagrangian method of analysis is commonly used to describe the process. Particle trajectory is calculated from the generalized Besset-Boussinesqu-Ossen equation, which in its simplified form is reduced to the following expression:

$$m\frac{dv}{dt} = F^{(D)}+F^{(ext)}+F^{(R)} \tag{6}$$

2.3.1. Single particle motion model

Foundations of the Brownian Dynamics were established by Chandrasekhar (1943) for a Stokesian particle in a stationary fluid and for a force-free field. In this work an extension of BD for the case of moving fluid at the presence of external forces derived by Podgórski (2002) was used. The model takes into account Brownian motion, inertial effects, convection in a fluid and external forces. Integration of Equation (6) for the time interval Δt, small enough so that the host fluid velocity u_i and the external force $F_i^{(ext)}$ may be assumed constant over $(t, t+\Delta t)$, gives the following bivariate normal density probability distribution functions $\varphi_i(\Delta v_i, \Delta L_i)$ that during the time interval Δt the particle will change its i^{th} component of velocity by Δv_i and it will be displaced by the distance ΔL_i in i^{th} direction.

$$\varphi_i(\Delta v_i, \Delta L_i) = \frac{1}{2\pi\sigma_{vi}\sigma_{Li}\sqrt{1-\rho_c^{\,2}}}\exp\left\{-\frac{1}{2(1-\rho_c)^2}\left[\left(\frac{\Delta v_i - <\Delta v_i>}{\sigma_{Li}}\right)-\right.\right.$$
$$\left.\left.-\frac{2\rho_c(\Delta v_i - <\Delta v_i>)(\Delta L_i - <\Delta L_i>)}{\sigma_{vi}\sigma_{Li}}+\left(\frac{\Delta L_i - <\Delta L_i>}{\sigma_{Li}}\right)^2\right]\right\} \tag{7}$$

The generalized algorithm for the Brownian dynamics can be formulated as follows. For a given initial particle position and its initial velocity components, v_i, at the moment t, we calculate the local fluid velocity, u_i, the external forces, $F_i^{(ext)}$, then, we find the expected values $<\Delta v_i>$ and $<\Delta L_i>$ and the correlation coefficient, ρ_c. Next, we generate two independent random values G_{Li}, G_{vi}, having the Gaussian distribution with zero mean and unit variance. Finally, we calculate the change of particle velocity, Δv_i, and the particle linear displacement, ΔL_i, during the time stem Δt from the expressions accounting for deterministic and stochastic motion.

All the steps are repeated for each co-ordinate i = 1, 2, 3. Having determined the increments Δv_i and ΔL_i the new particle velocity at the moment $t + \Delta t$ is obtained as $v_i(t+\Delta t) = v_i+\Delta v_i$, and in the same manner the new particle position is calculated. After completing one time-step of simulations, the next step is performed in the same way.

2.3.2. Aggregate motion model

The aggregate motion model was developed by Moskal and Payatakes (2006). Transitional and rotational trajectory equations were estimated using Beer and Johnson (1997) approach. We assume that the same forces that act on single particles act on aggregates (Eq. 6) and that the only external force is the gravitational one.

The effective Brownian force in the Langevin equation is usually assumed to be a Gaussian "white noise" random process (Chandrasekhar, 1943; Gupta and Peters, 1985; Uhlenbeck and Ornstein, 1930). Of course, in order for the effective Brownian force to have the same overall effect as the actual Brownian force (which is exerted by the molecules), it should have the appropriate spectral intensity and acceleration characteristics. Iwan and Mason (1980) developed an equivalent linearization method for systems which are subjected to a non-stationary random excitation, and their findings were used by Abuzeid et al. (1991) and Chen, et al. (2002) to study processes involving Brownian dynamics. Based on the above, the Brownian force $F^{(B)}$, which is exerted on the i^{th} particle of the aggregate, is given by:

$$F^{(B)_i} = m_i \alpha_{Be} Z_i \tag{8}$$

where α_{Be} is defined as the characteristic magnitude of the acceleration of the Brownian excitation and $\boldsymbol{Z}_i$ is a dimensionless vector with random direction

$$\alpha_{Be} = \sqrt{\frac{432 \mu k_B T}{\pi d_p^{\,2} \rho_p^{\,2} C_s \Delta t}} \tag{9}$$

where Δt is the time step which is used in the simulation of the Brownian excitation and which is set equal to the time step used in the numerical integration of the trajectory equations.

The net Brownian force acting on an aggregate is the vector sum of the Brownian forces acting on all the primary particles, which form the aggregate. Here, by primary particle we understand the single, spherical particles forming the aggregate. However, it is clear that the Brownian force acting on a primary particle in an aggregate is smaller than that acting on a solitary primary particle. One reason is that a particle in an aggregate is shielded by its neighbors. The second reason is that fluid molecules have a relatively small probability of hitting points in particle-to-particle contact regions. Here, we will assume that the structure of aggregates is sufficiently open to make shielding by neighbors negligible. In order to take into account the particle-to-particle contact effect, we introduce an "accessibility" factor into Eq. (8)

$$F^{(B)}{}_i = m_i \alpha_{Be} f_{sh,i} Z_i \tag{10}$$

which is estimated by calculating the "accessible" area fraction $f_{sh,i}$ A simple approximate analytical expression was developed which estimates the drag force for each primary particle in an aggregate as a function of the number of its immediate neighbors. The translational and rotational motion of any aggregate of a given size, overall shape and internal structure is calculated through the numerical integration of a system of differential equations which describe the conservation laws of linear and angular momentum, in a form which pertains to a rigid aggregate of identical primary particles. A detailed solution may be found elsewhere (Moskal and Payatakes, 2006).

2.4. Resuspension model

The resuspension model is based on data reported by Reeks et al. (1988) and Ziskind et al. (2000). The Authors assumed that the adhesion and elastic reaction forces can be described by an equation of harmonic movement with dumping effect. Extending the approach, one can assume that particle

interactions also have an oscillatory character. The displacement of a particle at a cluster attached to the neighboring particles can be expressed as follows

$$-kx - b\frac{dx}{dt} = m\frac{d^2x}{dt^2} \tag{11}$$

Equation (11) describes the energy-balanced oscillatory model. The stiffness coefficient and dumping coefficient can be calculated from material properties of particles, surface and fluid (Przekop et. al, 2004). The re-entrainment occurs when the distance between the surfaces of bodies exceeds value (Ziskind et al., 2000).

$$y_b = 0.437\left(\frac{\pi^2\gamma^2 d_p/2}{\kappa^2}\right)^{\frac{1}{3}} \tag{12}$$

3. COMPUTATIONAL PROCEDURE

The models described above were used to simulate the deposition of spherical particles and aggregates in the system of constricted tube unit cells. Calculations were carried out for three different filters with the same thickness, l=15mm, and porosity, ε, but with different pore sizes (Table 1). The properties of the fluid and the particles are summarized in Table 2. The superficial fluid velocity was assumed to be 2.5 mm/s, which is a typical value used in water filters testing. The calculations were performed for Arizona ultrafine test dust. The particle size distribution is shown in Fig. 3. The properties of particles were assumed to be the same as those of SiO_2, which is the main component of Arizona test dust. The concentration of solid particles at the inlet was assumed to be c_0=100 mg/l.

Table 1. Porous medium parameters

	Filter 1	Filter 2	Filter 3
ε [-]	0.67	0.67	0.67
$R_1=R_2=h_0$ [μm]	30	15	6
r_c [μm]	21.5	10.6	4.3

Table 2. Fluid and solid particles properties

Suspension parameters
particles density, ρ_p = 2200 kg/m^3
water density, ρ = 997 kg/m^3
water viscosity, μ=0.89 mPas
work of adhesion, γ=0.1 J/m^2
Young's modulus, E=75 GPa
Poisson's ratio, ν=0.17

The plug flow was assumed at the inlet, which means that for all nodes at the inlet surface the equilibrium distribution with the assumed mean velocity was applied. At the outlet the no-stress conditions were applied, which was achieved by reproducing the same velocity distribution for the last 10 nodes in the main direction of the fluid flow. When a fluid particle enters a solidified site, it changes its moving direction for the opposite one. This method naturally leads to zero-velocity at the solid level. Solid particles, moving with the superficial fluid velocity, were uniformly distributed at the inlet. The

interactions between lattice-Boltzmann and Brownian dynamics were modeled as follows. Initially, the fluid velocity profile for a clean filter was calculated. Then the trajectories of aerosol particles with the time step of 10^{-8} s were tracked. The fluid velocity in a given point of space, necessary to calculate the drag forces acting on a particle, was determined as a superposition from the neighboring nodes. Obviously, the relation between the dimensionless velocity in the lattice-Boltzmann scheme and the physical one, used in Brownian Dynamics calculations, was linear. The displacement of single particles was calculated using the model described in Section 2.3.1, while displacement of aggregates by the model featured in Section 2.3.2 . The only external force assumed in calculations was the gravitational one. For the case of displacement of deposited particles additionally the adhesion force calculated from Eq. 13 was taken into account. If the moving particle touched the surface of collector or previously deposited particle, the deposition occurred. If the distance between the surfaces of deposited particles or particle and collector exceed the value calculated from Eq. 14 the resuspension took place. In case of deposition or resuspension of the particles, the geometry of the computational domain was changed and a new velocity profile was calculated. Additionally, if resuspension occurred to the cluster of particles, parameters of its shape and structure, necessary to solve aggregate motion model, were calculated.

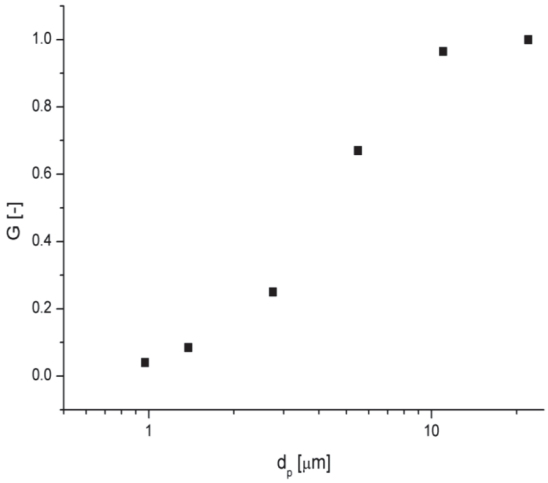

Fig. 3. Particles size distribution of ultrafine Arizona test dust

4. RESULTS AND DISCUSSION

The initial fractional efficiency of the filters is depicted in Fig. 4. Figs. 5 and 6 show the time evolution of filtration efficiency and pressure drop of the filters, respectively. The calculations were carried until the pressure drop reached the value 5 times higher than the initial pressure drop. For the biggest solid particles we can observe a drop of the filtration efficiency at some stages of the process, which is caused by particle resuspension. This phenomenon is especially visible at the later stages of filtration, when the presence of deposited matter leads to local increase of fluid velocity and thus produces higher stresses across the deposits. At the same time, large particles deposited on the smaller ones are the most tractable to resuspend into the fluid stream.

Figure 7 shows the time evolution of σ/ε ratio, were σ is the specific deposit (the apparent volume of deposited material per unit volume of the filter) vs. the depth of the filter. As can be seen during the early stages of filtration σ/ε decreases monotonically with depth, while for the later stages the maximum is observed at some distance from the filter surface, which is caused by the re-entrainment and redeposition of particle clusters. Recently Jackiewicz et al. (2015) reported similar behavior for experimental analysis of particles deposition in fibrous filters. This phenomenon was not observed by Skouras et al. (2004) in model work which neglected the possibility of particles reentrainment.

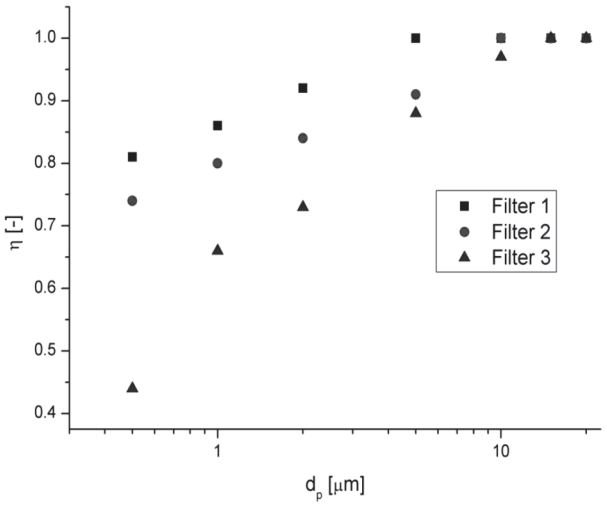

Fig. 4. Initial fractional efficiency

Fig. 8 shows the distribution of a number of primary particles in clusters resuspended to the fluid stream and counted at the outflow from the filter. As can be seen large clusters tend to redeposit at the deeper layers of the filter.

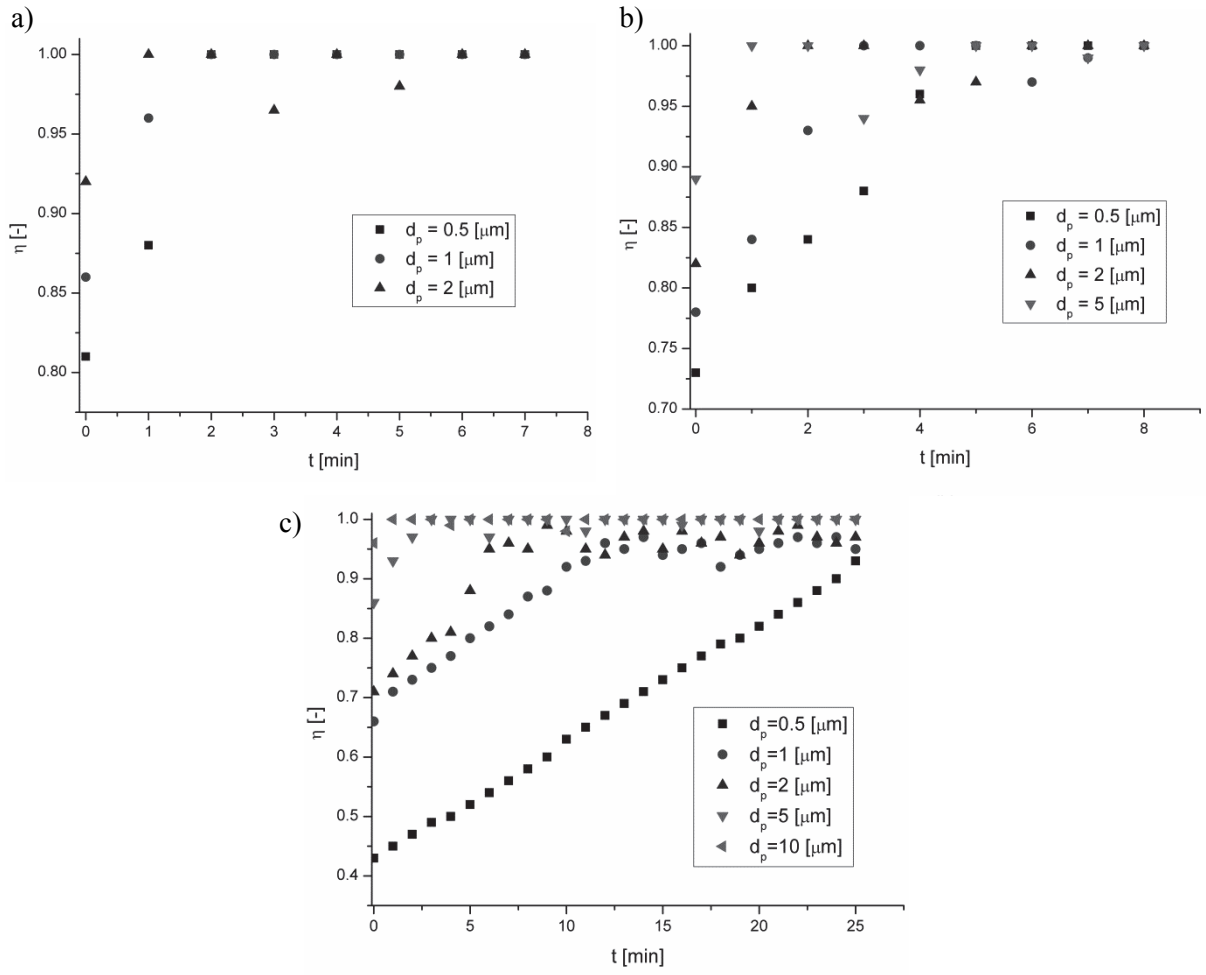

Fig. 5. The evolution of filter efficiencies, (a) Filter 1, (b) Filter 2, (c) Filter 3

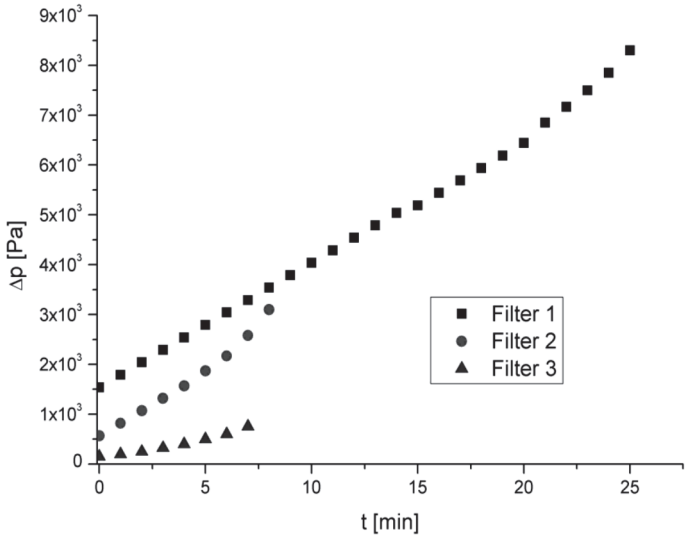

Fig. 6. Time evolution of pressure drop

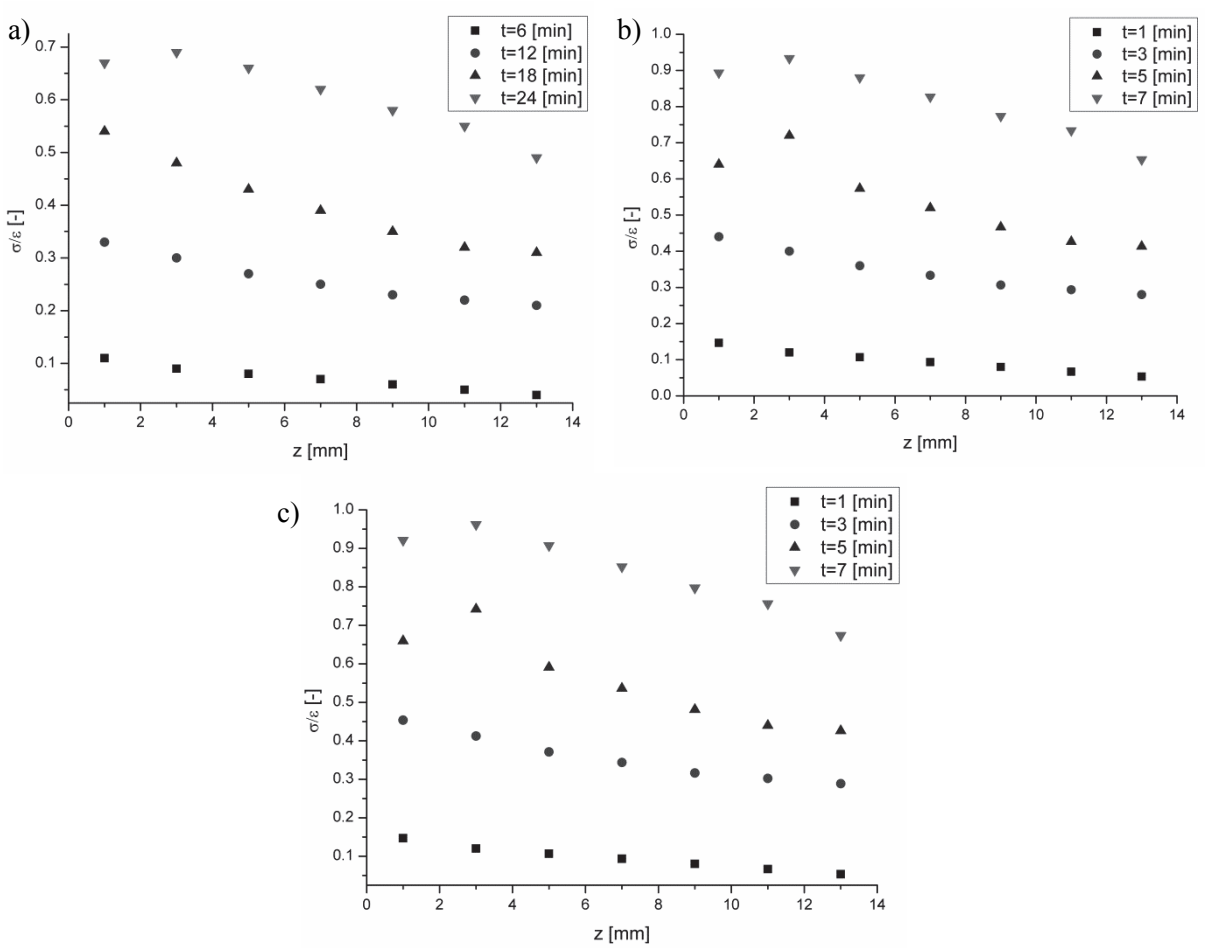

Fig. 7. Distribution of normalized specific deposit at various times, a) Filter 1, b) Filter 2, c) Filter 3

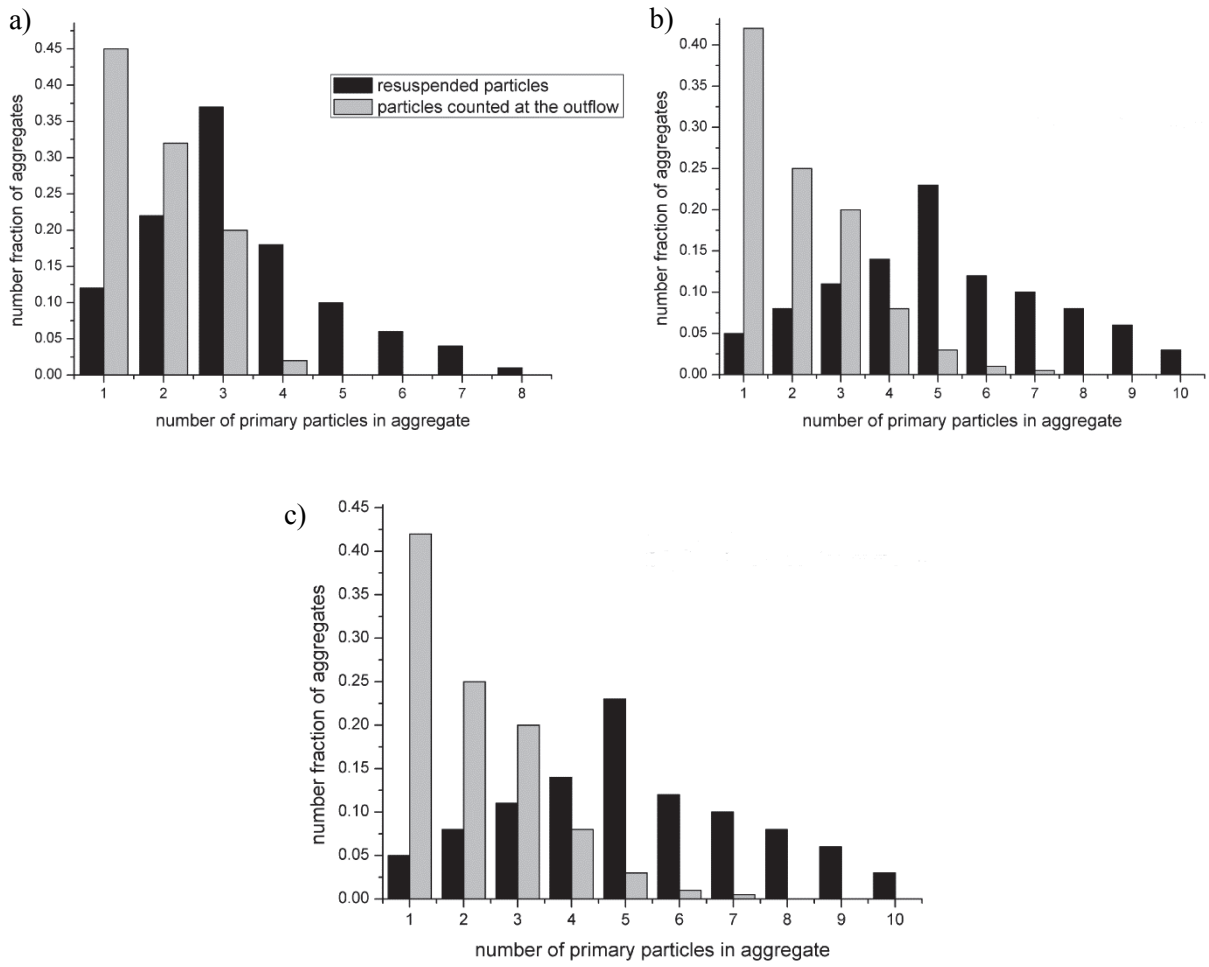

Fig. 8. Size distribution of aggregates

5. CONCLUSIONS

The simulations performed in this work cover all the key phenomena of deep bed filtration – initial filtration, the growth of deposits, re-entrainment and redeposition of clusters, possible clogging of pores. The dynamic behavior can be described not only by the evolution of deposition efficiency and pressure drop but also by the spatial distribution of deposits. The model enables prediction of dynamic filter behavior. It can be a very useful tool for designing filter structures which optimize maximum filter lifetime with the acceptable values of filtration efficiency and pressure drop. By using the Lagrangian approach of Brownian dynamics, the model avoids the problem of numerical instability, which was reported by Long and Hilpert (2009) for higher values of Peclet number.

This work was financed by Swiss Contribution, Polish-Swiss Research Programme number PSPB-209/2010.

SYMBOLS

b	dumping coefficient, kg/s
b_f	fluid dumping coefficient, kg/s

b_m	mechanical dumping coefficient, kg/s
c_0	particles concentration, mg/l
$\bar{c}_s$	dimensionless sound speed
C_s	Cunningham factor
d_p	diameter, m
e	unit vector
E	Young modulus, Pa
f	distribution function
f_{sh}	accessible area fraction
$F^{(D)}$	drag force, N
$F^{(ext)}$	external force, N
$F^{(R)}$	random Brownian force, N
g	acceleration of gravity
G_{vi}	random number
G_{Li}	random number
h	length of the tube, µm
k	stiffness coefficient, kg/s^2
k_B	Boltzmann constant, J/K
l	filter thickness, mm
L_i	displacement, m
m	mass, kg
P	pressure, Pa
r_c	radius in the narrowest cross-section of the tube , µm
R_1	radius of the inlet of the tube, µm
R_2	radius of the outlet of the tube, µm
t	time, s
$\bar{t}$	dimensionless time
T	temperature, K
u	fluid velocity, m/s
$\bar{u}$	dimensionless fluid velocity
v	particle velocity, m/s
x	position, m
$\bar{x}$	dimensionless position
y_b	distance between surfaces, m
Z	vector

Greek symbols

a_i	model constant
α_{Be}	characteristic magnitude of acceleration, m^2/s
γ	work of adhesion, J/m^2
ε	porosity
κ	elastic constant, Pa^{-1}
λ	mean free path, m
μ	viscosity, Pa*s
ν	Poisson's ratio
$\bar{\nu}$	dimensionless viscosity
ν_f	kinematic viscosity, m^2/s
ξ	coordination number
ρ	fluid density, kg/m^3
ρ_p	particle density, kg/m^3
$\bar{\rho}$	dimensionless density

ρ_c	correlation coefficient
σ	specific deposit
σ_{Li}	standard deviation of displacement, m
σ_{vi}	standard deviation of velocity, m/s
τ	relaxation time, s
$\bar{\tau}$	dimensionless relaxation time
ϕ	orientation angle, rad
ϕ_i	distribution function
Ω	collision term

REFERENCES

Abuzeid S., Busnaina A., Ahmadi G., 1991. Wall deposition of aerosol particles in a turbulent channel flow. *J. Aerosol Sci*., 22, 43–62. DOI: 10.1016/0021-8502(91)90092-V.

Beer F.P., Johnson Jr. E.R., 1997. *Vector mechanics for engineers dynamics*. 6th edition, McGrow-Hill, Boston.

Biggs M.J., Humby S.J., Buts A., Tuzun U., 2003. Explicit numerical simulation of suspension flow with deposition in porous media; influence of local flow field on deposition processes predicted by trajectory methods. *Chem. Eng. Sci*., 58, 1271-1288. DOI: 10.1016/S0009-2509(02)00103-3.

Chandrasekhar S., 1943. Stochastic Problems in Physics and Astronomy. *Rev. Mod. Phys*., 15, 1-89. DOI: 10.1103/RevModPhys.15.1.

Chen S., Cheung C.S., Chan C.K., Zhu C., 2002. Numerical simulation of aerosol collection in filters with staggered parallel rectangular fibres. *Comp. Mech.*, 28, 152–161. DOI: 10.1007/s00466-001-0289-4.

Dunnett S.J., Clement C.F., 2006. A numerical study of the effects of loading from diffusive deposition on the efficiency of fibrous filters. *J. Aerosol Sci*., 37, 1116-1139. DOI: 10.1016/j.jaerosci.2005.08.001.

Dunnett S.J., Clement C.F., 2012. Numerical investigation into the loading behavior of filters operating in the diffusional and interception deposition regimes. *J. Aerosol Sci.*, 53, 85-99. DOI: 1016/j.jaerosci.2012.06.008.

Gupta D., Peters M., 1985. A Brownian dynamics simulation of aerosol deposition onto spherical collectors. *J. Colloid Interface Sci*., 104, 375–389. DOI: 10.1016/0021-9797(85)90046-3.

Iwan D.W., Mason, Jr. B.A., 1980. Equivalent linearization for systems subjected to non-stationary random excitation. *Int. J. Non-Lin. Mech*. 15, 71–82. DOI: 10.1016/0020-7462(80)90001-3.

Jackiewicz A., Jakubiak S., Gradoń L., 2015. Analysis of the behavior of deposits in fibrous filters during non-steady state filtration using X-ray computed tomography. *Sep. Pur. Techn*., 156, 12-21. DOI: 10.1016/j.seppur.2015.10.004.

Karadimos A., Ocone R., 2003. The effect of the flow field recalculation on fibrous filter loading: a numerical simulation. *Powder Techn.*, 137, 109-119. DOI: 10.1016/S0032-5910(03)00132-3.

Long W., Hilpert M., 2009. A correlation for the collection efficiency of Brownian particles in clean bed filtration in sphere packings by a lattice-Boltzmann method. *Environ. Sci. Technol.*, 35, 205-218. DOI**:** 10.1021/es8024275.

Masselot A., 2000. *A new numerical approach to snow transport and deposition by wind: A parallel lattice gas model*. PhD Thesis, Geneve University, 2000.

Moskal A., Payatakes A.C., 2006. Estimation of the diffusion coefficient of aerosol particle aggregates using Brownian simulation in the continuum regime. *J. Aerosol Sci*., 37, 1081-1101. DOI: 10.1016/j.jaerosci.2005.10.005.

Payatakes A.C., Tien C., Turain R.M., 1973. A new model for granular porous media: Part I. Model formulation. *AIChE J*., 19, 58-67. DOI: 10.1002/aic.690190110.

Podgórski A., 2002. *On the transport, deposition and filtration of aerosol particles in fibrous filters: Selected problems*. Oficyna Wydawnicza Politechniki Warszawskiej, Warsaw.

Przekop R., Gradoń L., 2008. Deposition and filtration of nanoparticles in the composites of nano- and microsized fibers. *Aerosol Sci. Techn.*, 42, 483-493. DOI: 10.1080/02786820802187077.

Przekop R., Grzybowski K., Gradoń L., 2004. Energy-balanced oscillatory model for description of particles deposition and reentrainment on fiber collector. *Aerosol Sci. Techn.*, 38, 330-337. DOI: 10.1080/02786820490427669.

Przekop R., Podgórski A., 2004. Effect of shadowing on deposition efficiency and dendrites morphology in fibrous filters. *Chem. Process Eng.*, 25, 1563-1568.

Qian Y.H., d'Humieres D., Lallemand P., 1992. Lattice-BGK models for Navier-Stokes equation. *Europhys. Lett*., 17, 479–484.

Reeks M.W., Reed J., Hall D., 1988. On the resuspension of small particles by turbulent flow. *J. Phys. D*., 21, 574-589.

Skouras E.D., Burganos V.N., Paraskeva C.A., Payatakes A.C., 2004. Simulation of downflow and upflow depth filtration of non-Brownian particles under constant flowrate or constant pressure drop. *J. Chinese Inst. Chem. Eng*., 35, 87-100.

Sztuk E., Przekop R., Gradoń L., 2012. Brownian dynamics for calculation of the single fiber deposition efficiency of submicron particles. *Chem. Process Eng.*, 33, 279-290. DOI: 10.2478/v10176-012-0025-y.

Uhlenbeck E.G., Ornstein S.L., 1930. On the theory of the Brownian motion. *Phys. Rev*. 36, 823–841. DOI: 10.1103/PhysRev.36.823.

Wang Q., Maze B., Vahedi Tafreshi H., Pourdeyhimi B., 2006. A case study of simulating submicron aerosol filtration via lightweight spun-bonded filter media. *Chem. Eng. Sci*., 61, 4871-4883. DOI: 10.1016/j.ces.2006.03.039.

Ziskind G., Fichman M., Gutfinger C., 2000. Particle behavior on surfaces subjected to external excitations. *J. Aerosol Sci*., 26, 703-720. DOI: 10.1016/S0021-8502(99)00554-6.

Received 21 September 2015
Received in revised form 19 June 2016
Accepted 20 June 2016